Pakistan Journal of Engineering and Technology, PakJET
ISSN (p): 2664-2042, ISSN (e): 2664-2050
Volume: 5, Number: 2, Pages: 28- 35, Year: 2022

Design and Development of Bidirectional DC-DC Dual Active Bridge Converter for Energy Storage Systems

Nishankumar Rajendrabhai Patel[1], Junaid Rehman[2], Zuhaib Alam[3], Masroor Munsif Qureshi[4], Shubash Kumar[3]

[1] School of Electrical & Computer Engineering RMIT University, Melbourne Australia
[2] Muhammad Ali Jinnah University, Karachi, Pakistan
[3] Indus University, Karachi, Pakistan
[4] Central Queensland University, Sydney Campus, Australia

Received: 25/02/2022, Revised: 01/05/2022, Accepted: 25/05/2022

Abstract- The ever-increasing demand for renewable energy resources as compared to conventional means of energy generation has resulted in a growing demand for more efficient power storage systems and applications. However, this necessitates the use of different converters that must be employed to achieve efficient voltage conversions right from the generation stage to the point power is stored in the battery banks. To achieve efficient conversions of the voltage levels, Bidirectional DC-DC Dual-Active-Bridge (DAB) converters can be employed. Accordingly, this research work involves use of a closed-loop PI controller for controlling the outputs of a DC-DC converter and compensating for the load disturbances. The Simulink-derived results indicate the input & output characteristics of the converter to achieve the design of a controller that is capable of providing significant tracking reference command without undergoing steady-state error, thereby offering a fast transient response. Hence, by maximizing the performance of the converter, the controller resolves the issues identified in the output current. The system was also implemented on a 400W laboratory experimental model with a view to additionally validate its performance effectiveness. As a whole, a DAB system was successfully designed, simulated, implemented and analyzed for employing in various energy storage applications.

Index Terms
Dual-Active Bridge Converters, Closed-loop PI Controllers, Energy Storage Systems, Simulink Model.

I. INTRODUCTION

Energy is a vital requirement for achieving industrial progress and socio-economic prosperity. The modernization of the energy sector is indispensable for meeting the contemporary needs of the energy sector. The modern infrastructure used for the energy sector is based on smart grids that utilize microgrids for delivering electrical power to the loads of diverse nature [22-23]. The use of battery-based energy storage devices is crucial

in both residential and commercial applications. These devices also enhance the safety of electricity supply amidst peak demand of electricity by becoming an integral part of a micro-grid and thus provide a high level of power control capabilities [1-2]. As a result, a smart grid must be dependable and permit the integration of cleaner electrical energy resources like solar panels, wind turbines etc. However, because these energy-generating devices have varying electrical characteristics, their integration into a modern smart grid is a challenging task. Besides, to make intermediate energy smoothly flow between these devices, power electronic converters are required to achieve this purpose [3] [22]. An application of a bidirectional DAB converter is presented in Fig. 1. As discussed in [4], energy conversion systems include a galvanically-isolated DAB converters. The DAB converters are critical for integrating greener sources into the smart grid. During the normal or grid supported operations, bidirectional power flow is required to charge and discharge the battery. This is shown in figure 1. Furthermore, to regulate this complex power flow, a robust and high-performance control algorithm is required. To design and develop such a system, a bidirectional DAB converter is commonly employed. In [5], the authors explain how a DAB can be used to charge batteries in a plugged-in hybrid electric vehicle. In [6], to increase the practicality of the energy storage systems, the authors designed a half-bridge DC-DC converter based on coupled inductors. In addition, the authors used a DAB DC-DC converter to interface an ultra-capacitor microgrid applications [7].

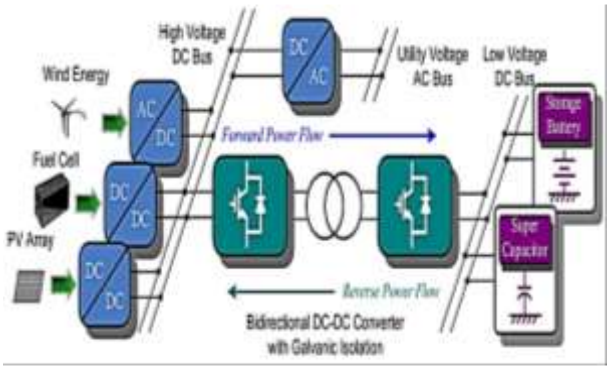

FIGURE 1: Application of bi-directional DAB in microgrid

Previous research on DAB DC-DC converters primarily focused on topology, control methods, and system modeling using the traditional methods. In [8], the authors presented a bidirectional switched capacitor based DC-DC converter having a current control mechanism. However, the operating modes, ripples in the output current at changing loads, the dead-band effect, and the issues governing the safety of operation were all the major concerns that were overlooked in the study.

In [9], the authors developed enhanced phase-shift control of bidirectional DAB for power distribution in a microgrid. The authors updated the calculation of zero-voltage switching for single and double pulse-width modulation controls for power transfer [10].

This work demonstrates the performance improvement of a bidirectional DAB converter. The DAB topology was chosen because it allowed for the DC-DC conversions with medium-to-high voltage and high-power based on a transformer with high frequency and bi-directional power flow. One of the key challenges in this conversion process was to investigate the closed-loop performance and create a high-performance closed-loop current regulator. In [11], an adaptive proportional-integral (PI) control of DAB was proposed which was mainly utilized for gain adjustment at operating points and various load conditions.

A sliding mode control of DAB encountered overshoots and steady-state errors [12-13] [23]. Later on, a double-integral sliding-mode controller was developed which demonstrated only a voltage regulation output of a DC-DC DAB converter [14]. Thus, this study was conducted to regulate and compensate for the output of a DC-DC DAB converter. For this purpose, a PI current mode controller was used to regulate the disturbances at source or load. To remove steady-state errors between the converter and its reference, the PI controller was employed. The converter's effective performance in DC output current was additionally demonstrated using a 400W I-phase laboratory model that took into account step changes in the reference current.

II. BASICS OF DUAL-ACTIVE BRIDGE CONVERTER

A dual-active bridge converter has quite simple principle of operation. A high-frequency AC connection connects two active H-bridge converters, which are subsequently phase-shifted to regulate the output power. The basic schematic diagram of a bidirectional DAB converter is given in Fig. 2. The DAB topology employs H-bridges that are operated at a certain switching frequency, resulting in a square-wave voltage having a duty cycle of 0.5 [9]. The output power equation of the converter is given below.

$$P = \frac{V_1 V_2}{2\pi^2 fsLN}\varphi(\pi\text{-}|\varphi|)$$

Here, the V_1 and V_2 are the converter's input & output voltages respectively, the N represents high frequency transformer ratio, L shows the leakage inductance, fs denotes the switching frequency, φ indicates the phase-shift between the two bridges and (φ/π) is the ratio of phase shifts.

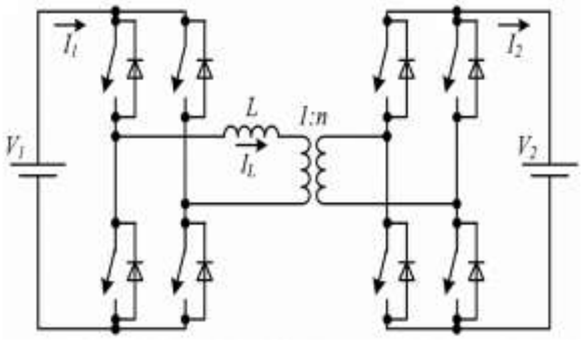

FIGURE 2: DC-DC DAB Converter (I-Phase)

The results given in Fig. 3 for the transformer primary & secondary voltage waveforms demonstrate that when the transformer input & output voltage ratio is the same as that of the converter corresponding ratio, the DAB converter supports higher efficiency [10].

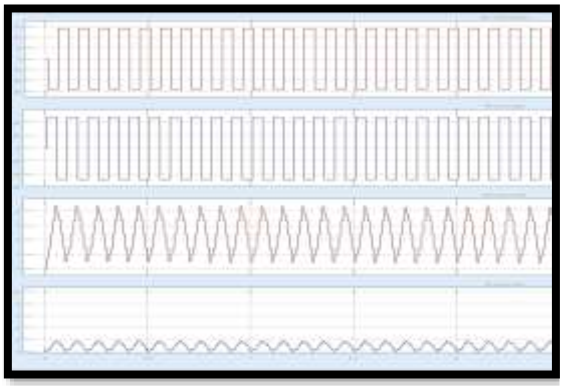

FIGURE 3: Output waveforms of DAB

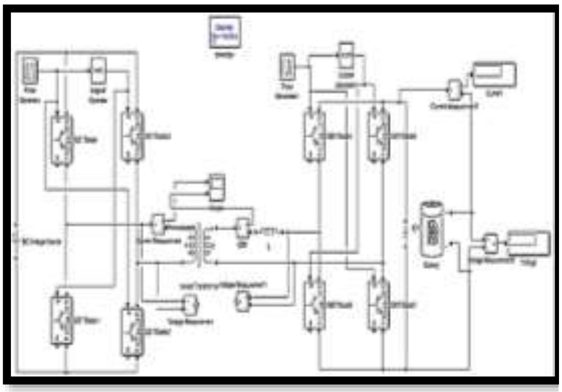

FIGURE 4: Phase shift square wave modulation

Needless to say, the two commonly applied key modulation schemes are Pulse-Width Modulation (PWM) and Phase-Shifted Square-Wave Modulation (PSSWM), the PSSWM method is widely accepted for providing the swiftest transient response. The PWM signal is produced by varying duty cycle of phase-leg of the bridge converter in a manner that the difference between the two waveforms occurs at the output terminal of the converter. The 2-level PSSW modulation is shown in Fig. 4 and 5. It shows a shift in both fixed-width pulses of high frequency at a duty cycle of 50% as opposed to the 3-level modulation, whose duty ratio is variable [1].

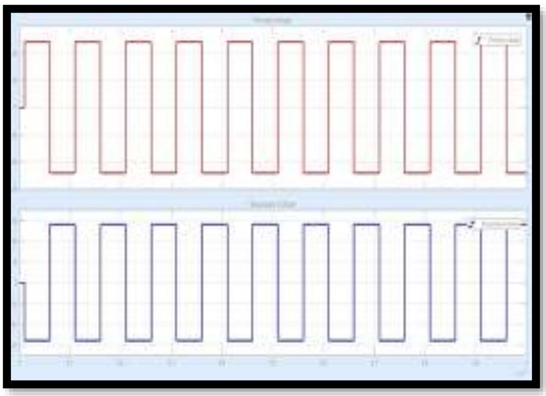

FIGURE 5: Square Waveform at 50% Duty Cycle of Phase Shift

Dual-Active Bridge-Converter Calculation

V_{DC} = 12 V

$V_{BATTERY}$ = 24V

Frequency (Switching) = 10 KHz

Buck & Boost modes can be both used to operate DAB.

Operation in Buck-Mode.

Duty Cycle $D = \frac{V_{BATTERY}}{V_{DC}} = \frac{24}{48} = 50\%$

Operation in Boost Mode

Duty Cycle D = 1- D_{Buck}= 50%

Three-level pulse width modulation may be accomplished using this mathematical approach. [13].

III. CONTROL METHODS

A PI controller is used in the regulation of current in a closed-loop system. A Simulink model of an open-loop controller is shown in Fig. 6. Although open-loop regulation initially helps resolve the control problem but it has its own limitations. The open-loop control cannot provide consistent performance at varying operating conditions as at some points of load transients, its performance is likewise ineffective, and thus it is not suited for achieving the proposed converter control mechanism [12] [23]. Therefore, obtaining the desired output from the DAB converter requires some pre-calculations which are done using the Look-up Table.

FIGURE 6: Open-loop controller Simulink model

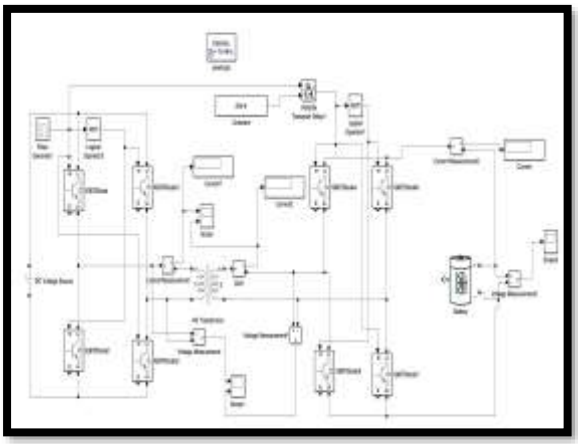

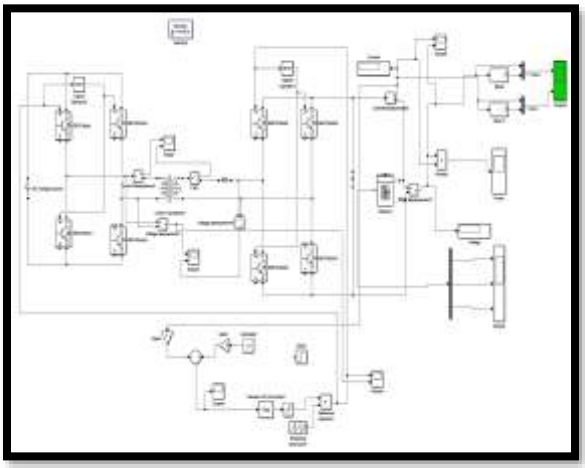

FIGURE 7: Simulink Model of Closed-loop PI controller

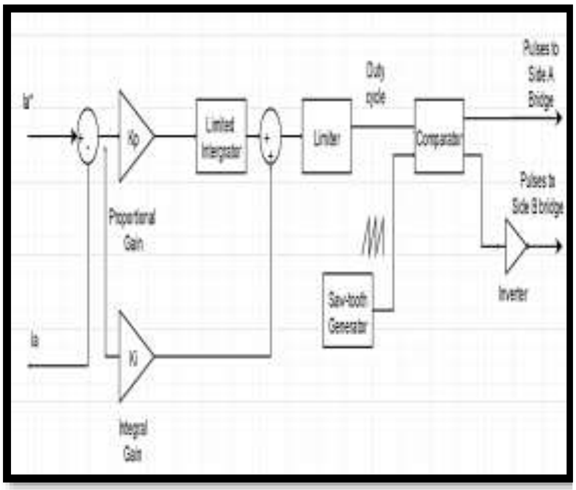

FIGURE 8: Overall block diagram of closed-loop PI controller

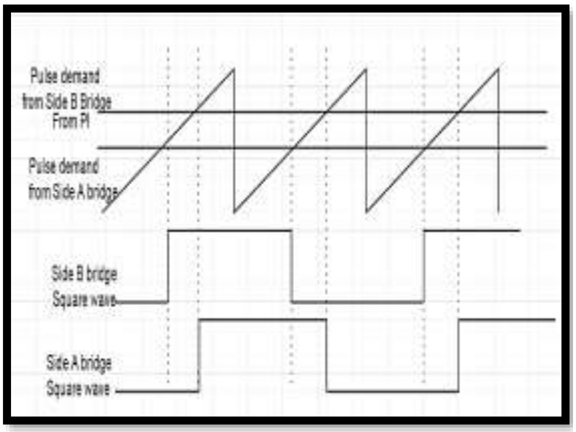

FIGURE 9: Basic concept of swift pattern

The basic closed-loop controller is shown in Fig. 7. DAB must be equipped with closed-loop regulation to be able to demonstrate good stability, fast transient recovery, and maintain desired output at different operating conditions. The two types of transients affecting converter performance are caused by load variation and reference command variation. The block diagram in Fig. 8 shows a PI based control technique for controlling the DAB converter. Using the comparator, the PI controller receives the error signal (by comparing the sampled & reference currents), which then calculates the phase-shift needed for the next modulation period. This is proportionate to the currents that were sampled and the currents that were used as the reference. In this system, a square wave generator was employed to generate two square waves for each converter bridge. The PI controller controls one of these signals, which is the side-A bridge, while the other is for the side-B bridge. This process is depicted in Fig. 9.

B. DAB Converter Control Structure

The gate signal in a DAB converter is regulated by its control structure. As a result, it performs two key tasks: reference command tracking and fast transient reaction with no steady-state error. The plant involves a DC link capacitor and resistance that are applied as convertor loads. The DC-link capacitor is parallelly positioned with the resistive load. These elements arranged as above offer appropriate loading conditions to the plant for calculating the reference command signal. Here, the representation of the Plant transfer function in Laplace domain is given by:

$$G(s) = \frac{1}{c(s) + \frac{1}{R(s)}}$$

According to the equation above, the plant must be able to control the DC quantity, which is the converter output current. A PI controller would suffice to deliver high-performance regulated output, and adequate tuning can provide steady-state accuracy. The PI controller transfer function is:

$$H(s) = Kp(1 + \frac{1}{Ti(s)}) \qquad [1]$$

The transfer function has been changed for the reference tracking component.

$$Io = Io\_ref\,\frac{H(s).G(s)}{1 + H(s).G(s)}$$

$$Io = Io\_ref\,\frac{Kp(Ti(s) + 1}{Ti.C.s^2 + Kp(Ti.s + 1)}$$

Where, $Ti = -\frac{1}{Tp}$

$$Tp = -\frac{1}{Rload * C}$$

After simplifying equation

$$Io = I_{ref}\,\frac{Kp * C}{s + Kp * C}$$

As Proportional Gain

$$Kp = 2 \times \pi \times Bandwidth \times C$$

Additionally, Integral Gain

$$Ti = -\frac{1}{Rload * C} = R \times C$$

Circuit Parameters	Value
Inductance (L1)	$25\mu H$
Inductance (L2)	$6.5\mu H$
Primary Turns (N1)	72
Secondary Turns(N2)	36
Turn Ratio	2: 1
V_{DC}	$48V$
BATTERY	$24V$
Switching Frequency	$10KHz$
DC-Link Capacitor	$1000\mu F$
Battery Resistance	$0.1212\ Approx.$
Phase Margin (φm)	50%
Proportional Gain (Kp)	0.3145
Integral Gain (Ti)	$1.21e^{-4}$
Bandwidth	$50Hz$

Lookup Table

IV. LABORATORY MODEL: TESTING, NALYSIS & RESULTS

To achieve the reliability and performance effectiveness of the DAB converter, a 400W laboratory model was developed but because of the software related complexities and the time constraints, programming the controller into the microcontroller was not possible. The control model of the DAB was developed using the embedded coder support package of Texas Instrument in the MATLAB Simulink and the microcontroller was programmed by code compose studio. Figure 10 presents the setup for the DAB converter.

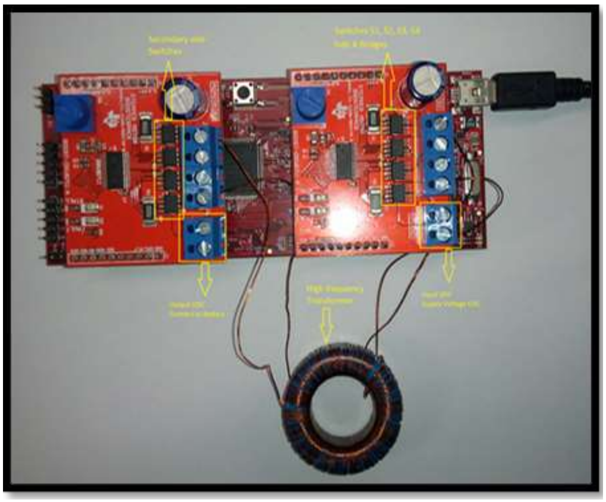

FIGURE 10: The DAB Converter

Figure 11 depicts the high-frequency current of the transformer. Transients in transformer current do not exist in the experimental data with the PI controller. The primary current is represented by the blue signal, while the secondary current is represented by the red signal.

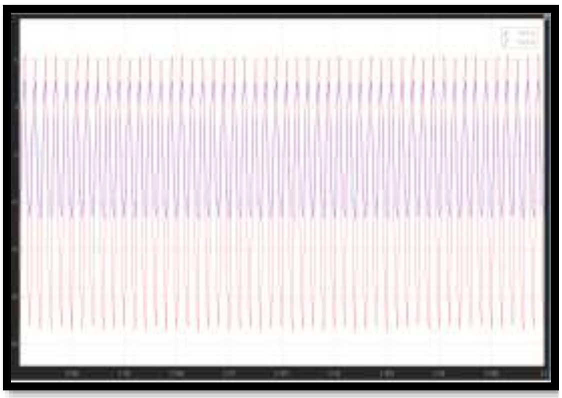

FIGURE 11: Transformer current primary and secondary

When feedback control is enabled, the converter outputs by controlling the phase-angle between voltages V1 & V2. The PI controller then calculates the error proportion and regulates the phase shift. Both sides of the bridges get the controlled signal. The phase angle of these two bridges changes as the load changes and the output load determines the phase angle of these two bridges.

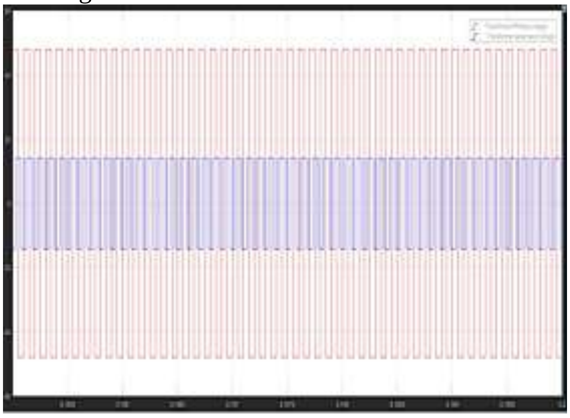

FIGURE 12: Shifted Pulses of Two Bridges

As shown in Fig. 12, toggling the PI controller's output produces the regulated gate pulses. The square-wave generator signal is then compared to the gate pulses. When the two independent gate pulses are controlled on either side of bridges, the red signal provides commands to four gate switches at primary side, while the blue signal gives commands to the switches at secondary side of the bridge. This can be seen in Fig. 13.

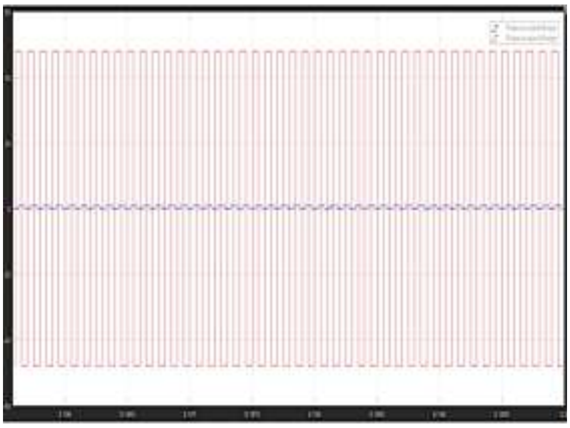

FIGURE 13: Square wave for either side of bridges

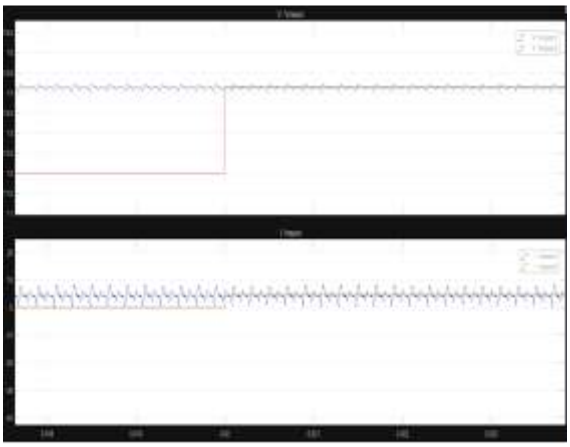

FIGURE 14: Output current of reference tracking

On a 5A rise in both reference commands, Fig. 14 shows the controller's current response and output voltage. As given in the diagram, the system output current and voltage both track the required reference with no steady-state errors.

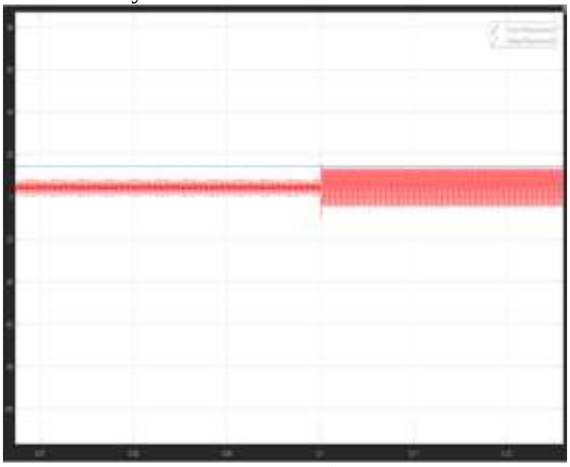
FIGURE 15: Step output of output current

In the Fig. 15, the converter output current is shown. Step modifications from beginning value 5 to final value 10 are given by the converter's reference command, indicating that the converter has calculated and compensated for the necessary phase shift to reach the reference value.

V. CONCLUSION & CONTRIBUTION

This research examined the performance analysis and effectiveness of bidirectional DAB converter in the design of energy storage systems. The results demonstrated adequate capability of the suggested converter in producing a consistent output against a set reference value. The system was successfully implemented and tested using the required component sizing and specifications, and in this regard, the parameters like error profiles, control schemes and performance requirements (in particular the voltage conversion efficiency) were evaluated using the simulation results. The controller performance was additionally verified using a 400W laboratory model after carefully performing thorough calculations and analyses. Overall, the findings show that the DAB converter provides strong performance control and operational reliability when subject to reference step changes or disturbances in high-end energy storage applications.

REFERENCES

[1] J. Leadbetter, and L. Swan, ‘Battery storage system for residential electricity peak demand shaving’, Energy and Buildings, vol. 55, pp. 685-692, Dec. 2012.

[2] Restrepo, A. Salazar, H. Schweizer, et al.: ‘Residential Battery Storage: Is the Timing Right?’ IEEE Electrification Magazine, vol. 3, no. 3, pp. 14 – 21, Sept. 2015.

[3] Segaran, D 2013, Dynamic modeling and control of dual active bridge bi-directional DC-DC converters for smart grid applications, Doctor of Philosophy (Ph.D.), Electrical and Computer Engineering, RMIT University.

[4] Andrei B., Roman K., Andrii C., Dmitri V.: ‘Bidirectional soft-switching dc-dc converter for battery energy storage systems’ IET Power Electronics, vol. 11, no. 12, pp/ 2000–2009, Oct. 2018.

[5] L. Xue, Z. Shen, D. Boroyevich, P. Mattavelli, and D. Diaz, "Dual Active Bridge-Based Battery Charger for Plug-in Hybrid Electric Vehicle With Charging Current Containing Low-Frequency Ripple," in *IEEE Transactions on Power Electronics*, vol. 30, no. 12, pp. 7299-7307, Dec. 2015.

[6] Yong Z., Xu-Feng C., Chengliang Y., Si C.: ‘A soft-switching Bidirectional DC-DC Converter for the Battery Super-Capacitor Hybrid Energy Storage System’ IEEE trans. Industrial Electronics, vol. 65, no. 10, pp. 7856 – 7865, Oct. 2018.

[7] Furkan A., Yakup T., Bulent V.: "An Energy Management Strategy for a Concept Battery/Ultracapacitor Electric Vehicle With Improved Battery Life," *IEEE Trans. Transportation Electrification*, vo. 3, no.1, pp. 191-200, Mar. 2017.

[8] H. S. Chung, A. Ioinovici and Wai-Leung Cheung, "Generalized structure of bi-directional switched-capacitor DC/DC converters," in *IEEE Transactions on Circuits and Systems I: Fundamental Theory and Applications*, vol. 50, no. 6, pp. 743-753, June 2003.

[9] B. Zhao, Q. Yu, and W. Sun, "Extended-Phase-Shift Control of Isolated Bidirectional DC-DC Converter for Power Distribution in Microgrid," in *IEEE Transactions on Power Electronics*, vol. 27, no. 11, pp. 4667-4680, Nov. 2012

[10] M. H. Azmeer bin Ab Malek and H. Kakigano, "Fundamental study on control strategies to increase the efficiency of the dual active bridge DC-DC converter," *Industrial Electronics Society, IECON 2015 - 41st Annual Conference of the IEEE*, Yokohama, 2015, pp. 001073-001078.

[11] Segaran D., McGrath B.P., Holmes D.G.: ‘Adaptive dynamic control of a bi-directional DC-DC converter’ in Proc. IEEE Energy Convers. Congr. Expo, pp.1442 -1449 2010.

[12] M. J. Carrizosa, A. Benchaib, P. Alou, G. Damm, ‘DC transformer for DC/DC connection in HVDC network’ in Proc. 15th Eur. Conf. Power Electron. Appl., pp.1-10, 2013.

[13] S. Talbi, A. M. Mabwe, and A. E. Hajjaji, "Control of a bidirectional dual active bridge converter for charge and discharge of a Li-Ion Battery," in Proc. of IEEE 41st Ann. IEEE-IECON, 2015, pp. 849-856.

[14] Y. C. Jeung, I. C. Choi, and D. C. Lee. "Robust voltage control of dual active bridge DC-DC converters using sliding mode control." in Proc. IEEE IPEMC-ECCE Asia, pp. 629-634, 2016.

[15] A. Rodríguez Alonso, J. Sebastian, D. G. Lamar, M. M. Hernando and A. Vazquez, "An overall study of a Dual Active Bridge for bidirectional DC/DC conversion," *IEEE Energy Conversion Congress and Exposition*, Atlanta, GA, 2010, pp. 1129-1135.

[16] G. Guidi, M. Pavlovsky, A. Kawamura, T. Imakubo and Y. Sasaki, "Improvement of light load efficiency of Dual Active Bridge DC-DC converter by using dual leakage transformer and variable frequency," *2010 IEEE Energy Conversion Congress and Exposition*, Atlanta, GA, 2010, pp. 830-837.

[17] M. N. Kheraluwala, R. W. Gascoigne, D. M. Divan, and E. D. Baumann, "Performance characterization of a high-power dual active bridge DC-to-DC converter," in *IEEE Transactions on Industry Applications*, vol. 28, no. 6, pp. 1294-1301, Nov/Dec 1992.

[18] R. W. A. A. De Doncker, D. M. Divan and M. H. Kheraluwala, "A three-phase soft-switched high-power-density DC/DC converter for high-power applications," in IEEE Transactions on Industry Applications, vol. 27, no. 1, pp. 63-73, Jan/Feb 1991

[19] H. Akagi and R. Kitada, "Control and Design of a Modular Multilevel Cascade BTB System Using Bidirectional Isolated DC/DC Converters," in IEEE Transactions on Power Electronics, vol. 26, no. 9, pp. 2457-2464, Sept. 2011.

[20] D. Holmes and T. Lipo, Pulse width modulation for power converters. Hoboken, NJ: John Wiley, 2003.

[21] H. R. Karshenas, H. Daneshpajooh, A. Safaee, A. Bakhshai, and P. Jain, "Basic families of medium-power soft-switched isolated bidirectional dc-dc converters," *Power Electronics, Drive Systems, and Technologies Conference (PEDSTC), 2011 2nd*, Tehran, 2011, pp. 92-97.

[22] M. Ahmadi and K. Shenai, "New, efficient, low-stress buck/boost bidirectional DC-DC converter," 2012 IEEE Energytech, 2012, pp. 1-6, doi: 10.1109/EnergyTech.2012.6304643.

[23] Khedr, M, Zeng, V & Pei, X 2021, Design of a Bidirectional DC/DC Converter for Energy Storage in Electric Aircraft. in 2021 IEEE Design Methodologies Conference (DMC)., 9529941, IEEE, U. S. A., pp. 1-6, IEEE Design Methodologies Conference (DMC) 2021, Bath, UK United Kingdom, 14/07/21. https://doi.org/10.1109/DMC51747.2021.9529941

ADDITIONAL SUPPORTING DIAGRAMS AND DESCRIPTIONS

For the AC link between the two bridges, the converter required a well-designed transformer. The design techniques are given below.

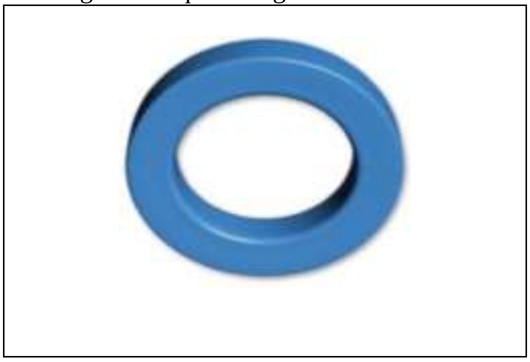

Figure 16: Cylindrical core of transformer (Toroid)

A microcontroller and I-phase Dual Active Bridge (DAB) kit was employed to complete this project. As a starting point,

Figure 17: Winding of transformer's core

the LAUNCHXL-F28069M from Texas Instruments was used to program the controllers because it had an onboard direct computer interface. Simulink embedded coder support package was used to develop a PI regulator in this microcontroller.

Figure 18: Launchpad Board

To control the gate signal of bridges, a I-phase step up and down regulator was required as shown in the figure below. Thus the BOOSTXL-DRV8305EVM was utilized as a Dual Active Bridge (DAB) Converter.

Figure 19: DAB Converter (I-Phase) with Four IGBT Switches

DATA SHEET OF CORE PARAMETERS

Inner Diameter = 20.5 mm
Outer Diameter = 34mm
Core Height = 12.5 mm
Length of Effective Magnetic Path = 82.06 mm
Effective Cross-Section Area = 82.6 mm^2
Inductance Factor A1 = 5.46 μH
Flux Density Optimum ΔB = 200 mT
Primary Turns Calculations.

$N1 = {}^{V * t}/_{\Delta B * Ae}$ = 72 Turns

Where V = 48V; t =25 μS

Voltage ratio 2:1 and the secondary turns are = 36 turns

Length of Primary Wire Mean = $\pi * D$ = 64.37 mm/turns

Mathematical Calculation of Inductance of the Transformer

Enamel Covered Wire = 25 SWG
Primary Inductance (L1) = 25 μH
Secondary Inductance (L2) = 6.5 μH

IMPORTANT ABBREVATIONS:

AC	Alternating Current
DAB	Dual Active Bridge
DC	Direct Current
f_s	Switching Frequency
K_i	Internal Gain
K_p	Proportional Gain
L	Leakage inductance
N	High-frequency transformer ratio
PI	Proportional Integral
PWM	Pulse Width Modulation
PSSWM	Phase-Shifted Square Wave Modulation
V_1	Converter Input Voltage
V_2	Converter Output Voltage
φ	phase shift